AGU PUBLICATIONS

Earth's Future

RESEARCH ARTICLE
10.1002/2016EF000500

Increasing transnational sea-ice exchange in a changing Arctic Ocean

Robert Newton[1], Stephanie Pfirman[1,2], Bruno Tremblay[1,3], and Patricia DeRepentigny[3]

[1]Lamont-Doherty Earth Observatory at Columbia University, Palisades, New York, USA, [2]Department of Environmental Science, Barnard College, New York, New York, USA, [3]Department of Atmospheric and Oceanic Sciences, McGill University, Montreal, Canada

Key Points:
- Ca. half of Arctic sea-ice melts within 100 km of formation, while ca. one fifth melts in a different nation's exclusive economic zone
- Over the past ca. 30 years, sea-ice drift speeds have increased and transit times decreased between remote parts of the continental shelf
- Exchange of sea ice and ice-rafted material between waters of the Arctic nations has likely increased over the past approximately 30 years.

Corresponding author:
R. Newton, bnewton@ldeo.columbia.edu

Citation:
Newton, R., S. Pfirman, B. Tremblay, and P. DeRepentigny (2017), Increasing transnational sea-ice exchange in a changing Arctic Ocean, *Earth's Future*, *5*, 633–647, doi:10.1002/2016EF000500.

Received 9 NOV 2016
Accepted 12 APR 2017
Accepted article online 26 APR 2017
Published online 27 JUN 2017

Abstract The changing Arctic sea-ice cover is likely to impact the trans-border exchange of sea ice between the exclusive economic zones (EEZs) of the Arctic nations, affecting the risk of ice-rafted contamination. We apply the Lagrangian Ice Tracking System (LITS) to identify sea-ice formation events and track sea ice to its melt locations. Most ice (52%) melts within 100 km of where it is formed; ca. 21% escapes from its EEZ. Thus, most contaminants will be released within an ice parcel's originating EEZ, while material carried by over 1 00,000 km^2 of ice—an area larger than France and Germany combined—will be released to other nations' waters. Between the periods 1988–1999 and 2000–2014, sea-ice formation increased by ~17% (roughly 6 million km^2 vs. 5 million km^2 annually). Melting peaks earlier; freeze-up begins later; and the central Arctic Ocean is more prominent in both formation and melt in the later period. The total area of ice transported between EEZs increased, while transit times decreased: for example, Russian ice reached melt locations in other nations' EEZs an average of 46% faster while North American ice reached destinations in Eurasian waters an average of 37% faster. Increased trans-border exchange is mainly a result of increased speed (~14% per decade), allowing first-year ice to escape the summer melt front, even as the front extends further north. Increased trans-border exchange over shorter times is bringing the EEZs of the Arctic nations closer together, which should be taken into account in policy development—including establishment of marine-protected areas.

Plain Language Summary We use data from satellite images to identify the formation, drift tracks, and melt locations of sea ice in the Arctic. Most ice melts locally: only about 21% is exported from the exclusive economic zone (EEZ) in which it is formed. That export is nonetheless about 1,000,000 km^2 each year. As the ice cover has thinned and the summer sea ice has retreated in a warming Arctic, formation and melt locations have moved further north, ice drifts have accelerated, and the area of ice formation and melt has increased. We looked at ice formation and transport between the EEZs of the Arctic nations, and broke the record into two periods: 1988–1999 and 2000–2014. As the Arctic warms, more ice is transported between EEZs and it is arriving at the receiving EEZ faster, than in the past. Between the two study periods: Sea ice velocity increased by about 14%/decade; Russian ice reached melt locations in other nations' EEZs 46% faster; and North American ice reached Eurasian destinations 37% faster. Exchanges of ice have increased as a result. For example, export of ice from Russia to Norway increased by 11% and export from Alaska to Russia by 16%.

1. Introduction

For stakeholders in the Arctic region, the transition to a seasonally ice-free ocean harbors both the possibility of economic development and growing risks [e.g., *Newton et al.*, 2016]. In no economic segment are rewards and risks more apparent than petrochemical extraction. The US Geological Survey estimates that about 90 billion barrels of oil, 1.7 trillion cubic feet of gas, and 44 billion barrels of natural gas liquids remain in the Arctic [*Bird et al.*, 2008; *Gautier et al.*, 2009] (Figure 1). About 84% of these resources lie beneath the Arctic Ocean and its peripheral seas, where accessibility is controlled primarily by the annual cycle in sea-ice growth, drift, and melt. The nightmare scenario is that when accidents occur, as they have in every major oil-field (Gulf of Mexico, Alaska, etc.), the extreme cold, seasonal darkness, remoteness, and presence of sea

ice will make containment and recovery extremely difficult, if not impossible [*Sørstrøm et al.*, 2010; *Harvey and Walker*, 2013]. *Blanken et al.* [2017], for example, found that sea ice will transport oil (and presumably other contaminants) significantly farther than ocean currents. The US National Academies of Science has recently completed a major study of the state of oil-spill management in the Arctic [*National Academies of Science* (*NAS*), 2014], and industry groups are investing in studies and experiments to develop response strategies [*Sørstrøm et al.*, 2010]. However, no technological solution currently exists to recover oil from sea ice, and a large fraction of the oil on, entangled in, or trapped beneath sea ice is likely to be transported with the floes and released into the ocean wherever the ice melts [*Venkatesh et al.*, 1990].

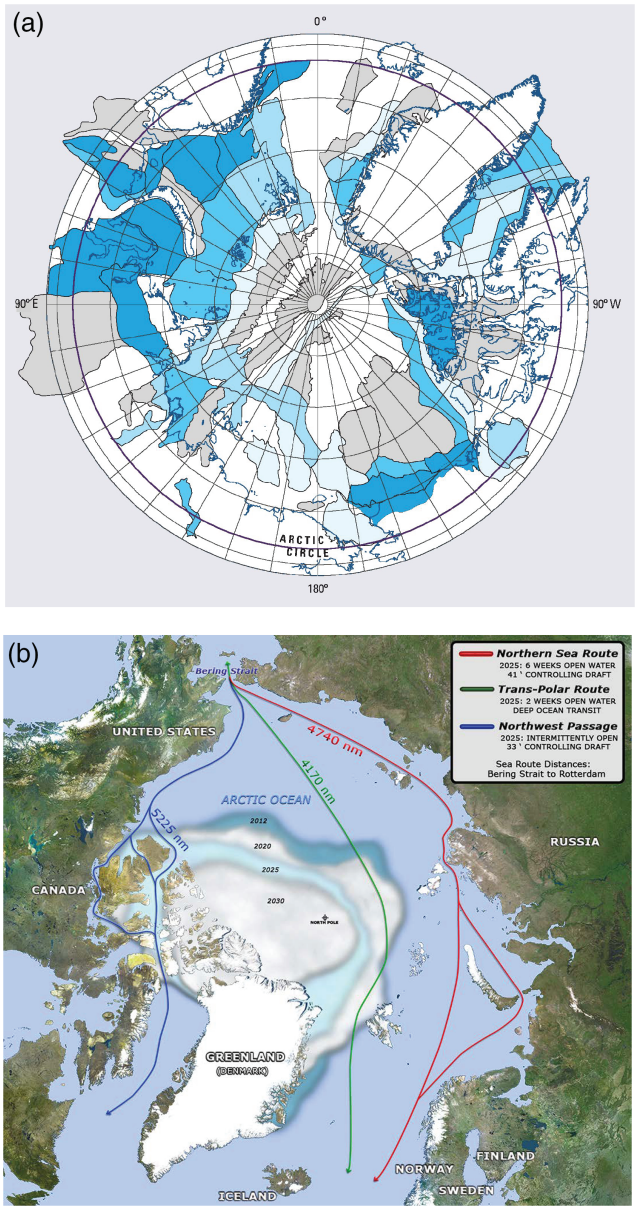

Figure 1. (a) Offshore oil and gas resources as assessed by the U.S. Geological Survey [*Bird et al.*, 2008]. (b) Summer sea ice extent minima and possible shipping routes (U.S. Navy: http://www.doncio.navy.mil/CHIPS/ArticleDetails.aspx?ID=5256).

For millions of years, sea ice has rafted material from one region of the Arctic Ocean to another: aeolian dust, aerosol deposits, sediments entrained in shallow waters, biological communities growing below each floe [e.g., *Pfirman et al.*, 1990; *Nürnberg et al.*, 1994; *Dethleff et al.*, 2000a; *Eicken et al.*, 1997, 2000; *Jakobsson et al.*, 2001]. Transport of the ice itself is a freshwater flux that moves buoyancy from source to sink regions, carrying river runoff, for example, from the Siberian shelf seas to the Canadian Basin [e.g., *Bauch et al.*, 1995; *Newton et al.*, 2008, 2013). Transport of biological communities, dust, and marine sediments may help to seed blooms at the retreating summer ice edge [e.g., *Meibing et al.*, 2007]. Ice-rafted sediments deposited over the central Arctic basin are read from benthic cores to document periods during the last several millions years when the Arctic was ice free or covered [e.g., *Bischof and Darby*, 1997; *Tremblay et al.*, 2015].

Beginning in the mid-19th century and accelerating through the 20th, industrialization in the far north added anthropogenic pollutants to the list of ice-rafted materials: mercury, lead, and other metals from mining and smelting operations, semi-volatile organic compounds and black carbon have all been observed on or in sea ice [e.g., *Pfirman et al.*, 1995; *Arctic Monitoring and Assessment Programme*, 1998, 2011, 2015; *Barrie et al.*, 1998; *Dethleff et al.*, 2000b; *Drozdowski et al.*, 2011; *Khelifa*, 2010; *Shevchenko et al.*, 2012]. As the Arctic warms, seasonally active marine transport for local delivery, trans-Arctic shipment and tourism is expected to grow quickly [*Khon et al.*, 2010; *Smith and Stephenson*, 2013, Figure 1b], which will lead to expanded port facilities and associated maritime and industrial activities along Arctic coasts. For example, the United States, Canada, and Russia are considering major infrastructure improvements along Arctic

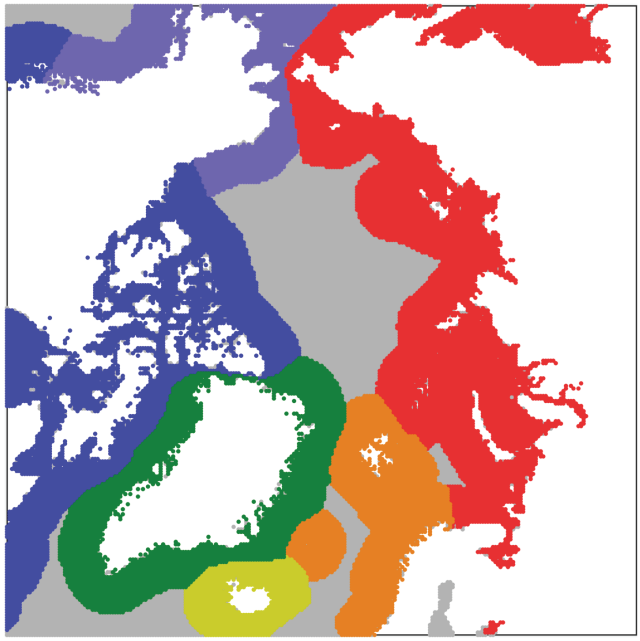

Figure 2. Arctic exclusive economic zones (EEZs).

coasts, including deep water porting and oil-spill response capacity [e.g., *DeCoste*, 2016; *Ruskin*, 2016; *State of Alaska*, 2016]. Marine infrastructure combined with longer and more extensive open-water periods, could expand the opportunities for extraction and processing of metals and minerals, accelerating pollution risks. Including the possibility of ice-rafting toxins from one region to another.

Sea ice receives pollutants from the atmosphere, water, or contaminated sea floor sediments, which are entrained if the water depth at the formation site is less than about 30 m. Despite these differences in their sources, the majority of pollutants are released when the entire floe melts [*Pfirman et al.*, 1995]. This occurs because most contaminants are particle reactive and even during summer ice melt are retained on the pitted, cryoconite-riddled surface of the floes [*Pfirman et al.*, 1995]. Also, for multi-year ice, over time, as ice melts from the surface and grows from the underside, contaminants migrate toward the floe surface [*Pfirman et al.*, 1995; *Tremblay et al.*, 2015]. Once released, contaminants will segregate based on their behavior in seawater. Particles and particle-reactive components will sink to the sea bed. Soluble components will follow the ocean currents. Long-lasting components may be re-entrained into ice the following fall. Melt regions sometimes coincide with algal blooms, and some contaminants are biologically active. The fate of contaminants after release is outside the scope of this contribution, but we note that the 2015 GEOTRACES cruises have gathered data that will address some of these issues in more detail than has been possible in the past.

Below we focus on the fate of sea ice itself, analyzing changes in regional ice transport rates. We take the exclusive economic zones (EEZ) of the Arctic nations (Figure 2) as our regional boundaries in order to directly connect our analysis of ice formation, transport, and melt patterns to policy frameworks. A nation's EEZ extends 200 nautical miles seaward from its coastline. EEZs are defined by the United Nations Convention on the Law of the Sea (UNCLOS), and disputes are resolved through UNCLOS processes. The United States, a major Arctic power, is not an UNCLOS signatory but has committed to abide by its processes. A comparison of Figures 1 and 2 shows that most oil and gas resources are located within EEZs, which roughly correspond to the continental shelves. The analysis presented below addresses the question: How has the exchange of sea ice between the EEZs of the Arctic nations changed in recent decades as the Arctic has warmed and summer sea-ice cover has decreased?

2. Methods

2.1. Input Data

The sea-ice motion data used in this study are from the Polar Pathfinder project, publicly available at the *National Snow and Ice Data Center (NSIDC)* website: https://nsidc.org/data/docs/daac/nsidc0116_icemotion.gd.html [*TSchudi et al.,* 2016]. The data set begins with the advent of polar-orbiting earth-observing satellites in late 1978. The drift fields are a gridded product derived through optimal interpolation of observations from the International Arctic Buoy Program (IABP) sea-ice buoys, and the Scanning Multi-channel Microwave Radiometer (SMMR), Special Sensor Microwave Imager (SSM/I), Special Sensor Microwave Imager Sounder (SSMIS), The Advanced Microwave Scanning Radiometer for EOS (AMSR-E), and Advanced Very High Resolution Radiometer (AVHRR) sensors, which have been mounted on a succession of National Oceanic and Atmospheric Administration (NOAA) and National Aeronautics and Space Administration

(NASA) satellite platforms starting in November, 1978. In places and times for which no satellite or buoy observations are available, sea ice "free drift" is calculated from the NCEP reanalysis surface wind estimates, using a simplified relationship between the geostrophic wind and ice motion [*Thorndike and Colony*, 1982]. The data are interpolated onto the 25 km Equal Area Scalable Earth (EASE-25) grid and is available in daily, weekly, and monthly mean fields. This study uses Version 3 of the weekly fields from 1988 to 2014.

The IABP buoy tracks are the most accurate Arctic sea-ice drift data; they are available at the IABP website: http://iabp.apl.washington.edu/. The NSIDC interpolation gives a large weight to buoys, which dominate the gridded velocities within a radius of influence of about 200 km. As background to this work, we compared satellite-derived drift estimates to buoy drifts whenever the two are approximately collocated (e.g., within 100 km) as a way to validate the accuracy of the satellite estimates. It is a method used as well by the NSIDC and others [*Schwegmann et al.*, 2011] to estimate error in the data set. We found that the SMMR data, the only satellite input between 1978 and mid-1987, is biased low compared to nearby buoys, which led to the removal of this section of the dataset from our analysis. The bias has been acknowledged by the NSIDC and may be related to the fact that the SMMR sampling period was 48 h, whereas for the other products, 24-h samples were used [*National Snow and Ice Data Center (NSIDC)*, 2016]. Thus, our study period is January 1988–December 2014.

The satellite-derived drift vectors are calculated by tracking features from one satellite image to the next [*Emery et al.*, 1991, 1995, 1997; *Fowler et al.,* 2003; *Kwok et al.*, 1998]. Successive images are geo-located, shifted by discrete pixel-widths up to 10 pixels, and compared. Two-dimensional cross-correlations are maximized to select a most-likely drift vector between images. Passive microwave instruments (SMMR, SSM/I, SSMIS, and AMSR-E) capture the electromagnetic radiation emitted by the surface. The AVHRR instrument captures sunlight reflected from the earth's surface as well as surface-emitted thermal infrared at about 11 μm wavelengths. Because the heights of polar orbiting satellites are similar (in the 700–850 km range), resolution is mainly governed by the frequency of radiation being captured, with higher frequencies providing greater spatial resolution. The 85–91 GHz microwave bands suffer more interference from atmospheric water than the lower frequency 37 GHz channel. Visible and infrared sensors give the best resolution (approx. 1.2 km/pixel). However, they have trouble distinguishing clouds from sea ice. In addition, reflected light is only available during about half the year when the sun is up [*Emery et al.*, 1995]. The same images that are used as grist for the pattern recognition software are used by the NSIDC to publish gridded estimates of sea-ice concentration—the fraction of each pixel covered by ice.

2.2. Lagrangian Ice Tracking System (LITS)

We have developed a Lagrangian Ice Tracking System (LITS) [*DeRepentigny et al.*, 2016; *Williams et al.*, 2016] that uses the NSIDC's Polar Pathfinder data to track ice floes from the location of their formation to where they ultimately melt. Here, we apply that software and the NSIDC data sets to study ice transport patterns, mainly by looking at the statistics of international transport and changes in those statistics and patterns with time. For each week during the satellite era, we identify ice formation events. To do so, one has to distinguish between ice that appears at a location through formation (freezing) and ice that arrives as a result of advection from a neighboring location. We advect each week's ice edge forward by a week, and compare the advected ice edge with the ice edge from satellite imagery. Ice-covered grid points that (1) were ice free in the previous week and (2) did not receive ice through advection are marked as formation events. Where a grid point has become ice covered through freezing, we identify a new ice "parcel" which is then advected forward in time, with weekly resolution, using the Polar Pathfinder ice drift velocity fields. We use 15% to define when a grid cell is inside the ice pack. Fifteen percent is widely used in sea-ice studies as the boundary of the ice pack and our own tests indicate that results are robust to the exact choice of cut-off value. For this study, the data set of weekly sea-ice maps was processed to identify all sea-ice formation events creating an array of the formation latitudes, longitudes, and dates. Then, LITS was seeded with all ice formation events, to create a data set of weekly locations of each "parcel" of ice. It is important to keep in mind that we are not identifying and tracking actual ice floes. Ice formation is a complex, nonlinear process that takes place on spatial scales much smaller than the 25 km grid spacing of the sea-ice data. Floes of significant size—the types that might be identifiable and trackable in satellite images—are built

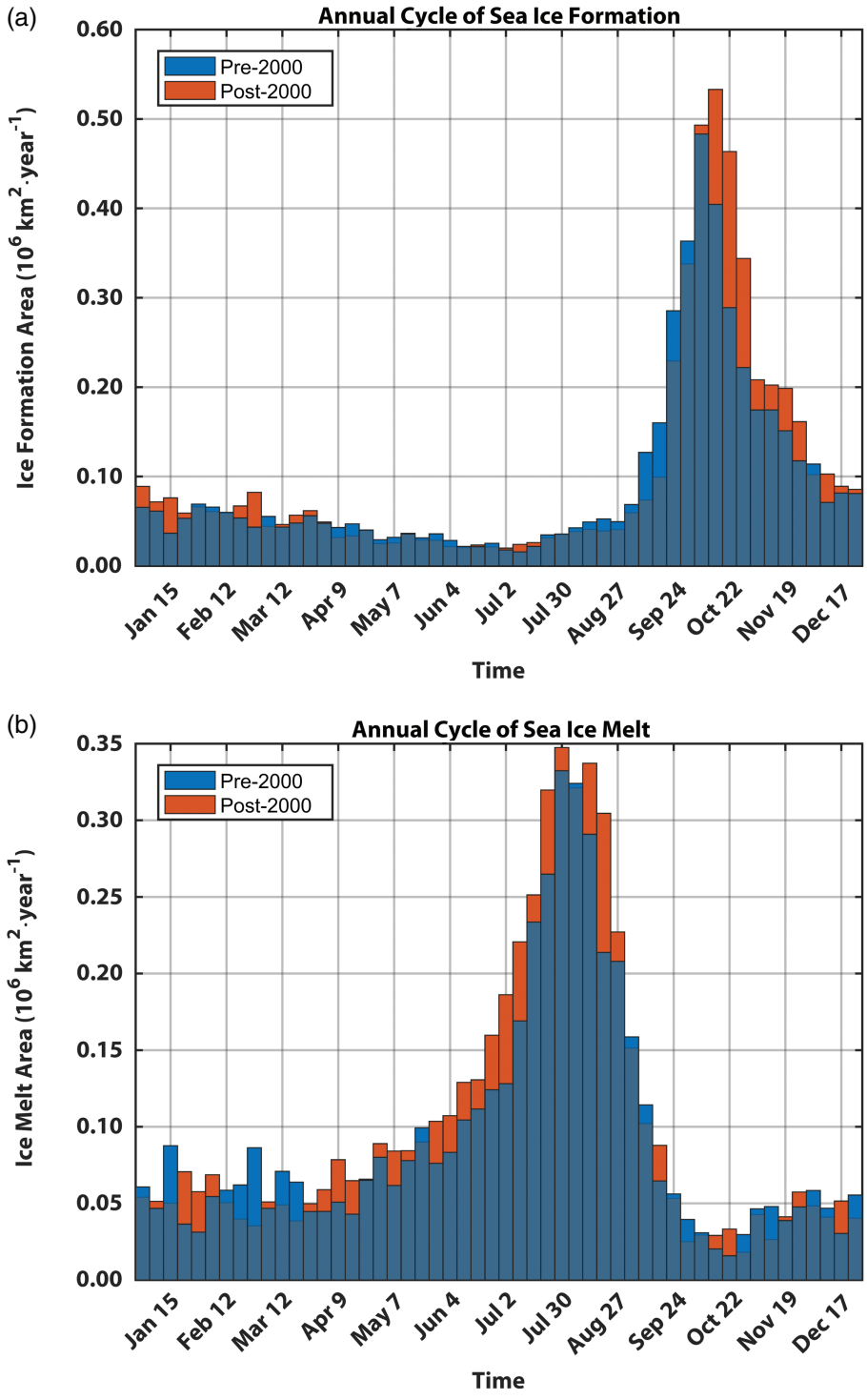

Figure 3. Annual cycle of sea-ice formation (a) and melt (b). Blue: 1988–1999. Orange: 2000–2014.

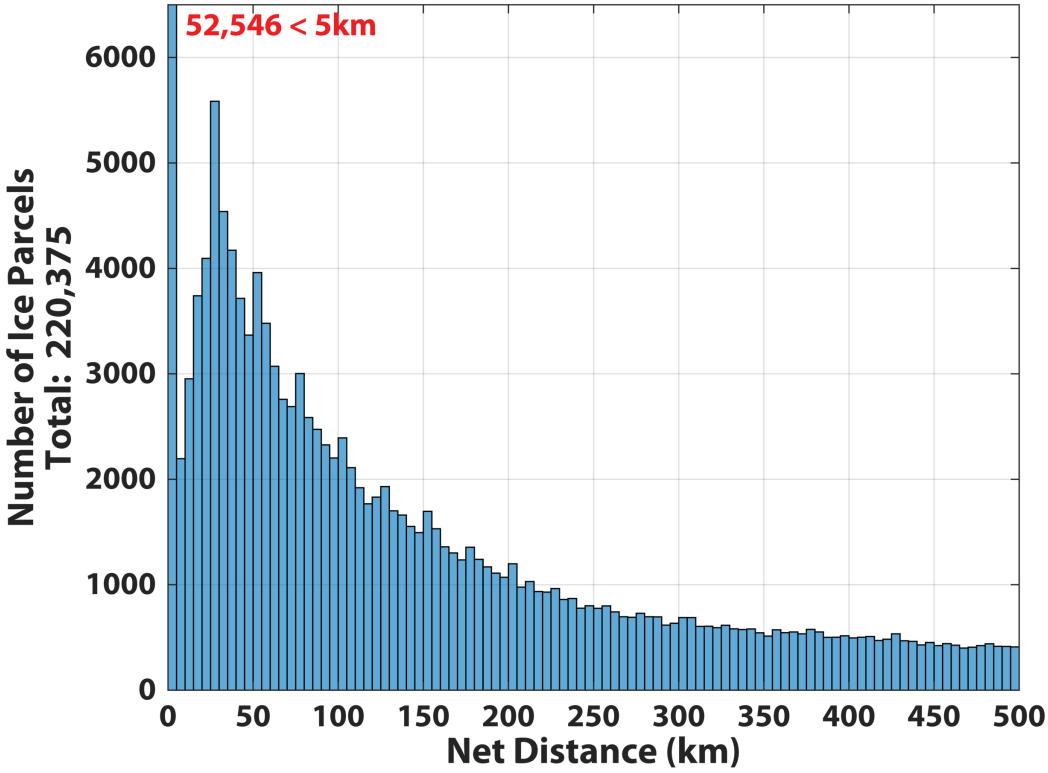

Figure 4. Net distance traveled (formation to melt site) by sea ice between 1988 WHY 1988? and 2014. The first bar, less than 5 km, represents ~24% of all parcels.

up over time by the concretion, continued vertical growth, and consolidation of already-formed ice. One can think of the tracked parcels as "virtual floes" or "buoys" that have been placed so as to be statistically representative of sea-ice creation events that lead to ice floes that last at least 1 week, the temporal resolution of the study. Each new ice parcel is tracked forward in time until it melts, with the intermediate locations and the melt location being saved to create an ice-drift track. Ice is considered to have melted when the location it should have arrived at is ice free.

In order to put sea-ice transport in a geopolitical context, the EEZ of formation and EEZ of melt were recorded along each parcel's track. Figure 2 shows the Arctic EEZs; the gray area in the center, not part of any nation's EEZ, is labeled "Central Arctic", and included in the formation/melt statistics. The study is restricted to formation events in the Central Arctic and its peripheral shelf seas, whereas the Nordic Seas and the East Greenland Current are included as melt regions, since that is where most ice exported from the Arctic is lost.

3. Results

3.1. Ice Formation and Melt

Between January 1, 1988 and December 31, 2014, the analysis identified 239,023 ice formation events in the study region. Each event places new ice at a grid point representing a 25 km × 25 km^2 – 625 km^2 of sea ice. Thus, we tracked an average of approximately 5.5 million square kilometers of sea ice formed each year. Figure 3 shows the annual cycle of formation (top) and melt (bottom) events averaged over 1988–1999 (blue) and 2000–2014 (orange). Before 2000, sea-ice formation increased sharply in the early fall, with a maximum in the second week in October of about 215,000 km^2/week, falling steadily through late October and November. By December, the Arctic Ocean is nearly completely ice covered and ice formation drops slowly to a minimum in early June. As the ice-edge approaches the coastlines in late fall, sea-ice formation is limited to coastal polynyas and the growth of ice area slows. Melting is more broadly distributed, with

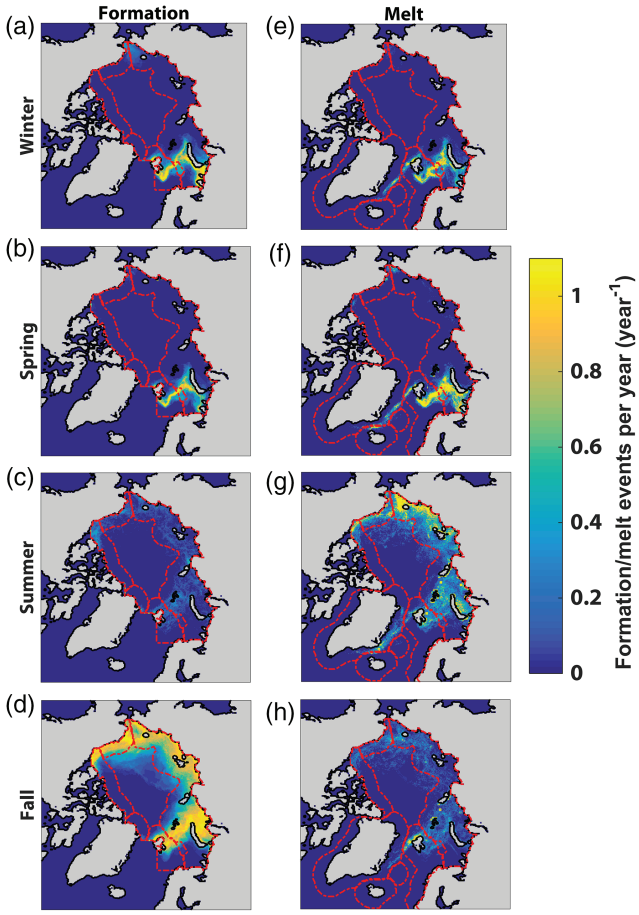

Figure 5. Annual density of sea-ice formation (left) and melt (right) for (top to bottom): winter (DJF), spring (MAM), summer (JJA) and fall (SON). Red lines are exclusive economic zones boundaries.

a peak of about 148,000 km^2/week in the first week of August and a steady, nearly linear decline between early-August and the minimum in mid-October.

After 2000, the annual cycles shift in ways congruent with a warmer Arctic atmosphere. Freeze-up begins and peaks about a week later on average than in the prior 12 years. Melt rises earlier and the peak period lasts longer, about 5 weeks instead of two. The areas of ice formation and melt are significantly larger, with peaks that are about 81,000 and 45,000 km^2 per week larger, respectively, than in the prior period. The larger annual cycle of formation and melt reflects the much larger area in the seasonal ice zone (SIZ—the area that is open in summer but ice covered in winter) as the summer ice cover retreats.

In July, at the peak in surface air temperatures, one would not expect significant sea-ice formation, yet our analysis shows about 10,000 km^2 formation per week. This is likely an expression of errors in the algorithm by which ice formation has been identified. Changes in sea-ice concentration maps are used to identify potential formation events, and ice drift is used to eliminate instances when ice was advected into a region. Most of the July ice formation occurs along coastlines where there are no buoy data and very few satellite-derived drift vectors, so that ice drift estimates are dominated by free drift calculated from the geostrophic wind. To the extent that the ice motions are inaccurate, ice can be identified as newly formed when in fact it has drifted into the area represented by a satellite image pixel. In addition, land-fast ice along the coast can be misidentified as floating sea ice. Assuming all of the July ice formation is spurious, and that errors in the drift and ice-edge location do not vary seasonally, then we estimate the errors on ice formation events to be approximately 4%. The impact on statistics of inter-EEZ exchange would be even less, as these isolated coastal parcels do not tend to persist very long.

Most sea-ice melts close to its formation location (distance distribution in Figure 4). Twenty-four percent of parcels melted essentially where they were formed (<5 km net drift) and 52% melted within 100 km; only approximately 17% of parcels traveled more than 500 km from their formation locations. 21.4% of ice melts outside of its EEZ of formation. While small compared to total sea-ice formation area, this nonetheless means that over 1 million km^2 of ice, an area larger than France and Germany combined, has been exported from one nation's EEZ to another's each year.

Figure 5 shows the spatial pattern of the sea-ice formation and melt rates, for each season, averaged over the 27-year data set. Autumn (Figure 5d) dominates the formation rates, with strong ice formation throughout the SIZ. There is some summer ice formation along the Siberian coast and a small amount throughout the continental shelf seas (Figure 5c). Some summer ice formation is real, but much of it represents errors in the LITS ice formation identification algorithm.

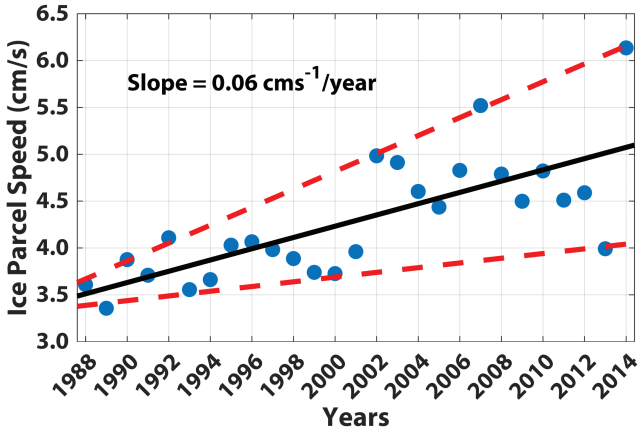

Figure 6. Annually averaged drift define red dashed curves speeds of sea-ice parcels that traveled more than 500 km from formation.

Table 1. Distribution of Sea-Ice Melt by the EEZ in Which It Was Formed, for Ice Tracked Between 1988 and 2014

To From	Canada %	USA %	Russia %	Norway %	Iceland %	Greenland %	Central %	Total km^2/yr
Canada	61.91	30.99	2.65	0.00	0.01	0.21	4.24	219,560
USA	0.40	47.31	45.19	0.00	0.09	1.22	5.78	443,403
Russia	0.05	0.10	86.54	7.46	0.70	4.05	1.10	3,224,699
Norway	0.00	0.00	0.08	99.28	0.01	0.63	0.00	647,407
Greenland	0.00	0.00	0.00	4.65	9.13	86.22	0.00	263,66
Central	1.67	8.62	23.27	6.05	3.41	18.29	38.70	198,356

EEZ, exclusive economic zones.
The last column is the annually averaged total area of ice formed in each EEZ.

In winter and spring, both ice formation (Figures 5a and 5b) and melt (Figures 5e and 5f) occur along the front where warm Atlantic and Pacific inflows meet cold Arctic surface waters. We interpret these events as mainly due to fluctuating atmospheric and, especially, oceanic fronts. Sea-ice melt takes place predominantly in the summer (Figure 5g). In the fall there is weak, but non-zero, melt over the Siberian shelf seas, some of which is real since melting still occurs at the beginning of September, but some of which likely represents errors in the melt-event identification algorithm, which relies on the accuracy of sea-ice drift estimates.

3.2. Transport Between EEZs

As the ice pack thins and retreats, it is more responsive to wind forcing and tends to move faster [*Rampal et al.*, 2009, 2011; *Spreen et al.*, 2011]. Focusing on floes that travel longer distances: we found that, for ice traveling more than 500 km, between 1988 and 2014, acceleration has been about 0.06 cm/s·year (about 14% per decade) (Figure 6). The acceleration rate has not been constant, and there are multi-year periods of higher acceleration, and deceleration. We checked to see whether the patterns of acceleration were related to the dominant mode of regional-scale atmospheric variability, the Arctic Oscillation, but the correlation was only 0.29, less than 10% of variance explained.

Of the ice that travels beyond its EEZ of origin, approximately one quarter exits the Arctic and melts in the Nordic Seas, in the EEZs of Greenland, Norway or Iceland, mainly in the East Greenland Current. The ice exported from Arctic EEZs, roughly 1 million km^2 annually, is certainly the largest international exchange of solid material on the planet, and potentially a major pathway for contaminants. Transport of the rafted material is complex, with additions and partial releases en route. Quantitative application to pollution transport will require a loading and release model, based on atmospheric conditions and location, which we have identified as important future development for the LITS.

Table 1 shows the distribution of melt locations by EEZ for each EEZ of formation. The data tracks 205,623 sea-ice parcels formed between 1988 and 2014 that had already melted by the end of 2014. Values are in

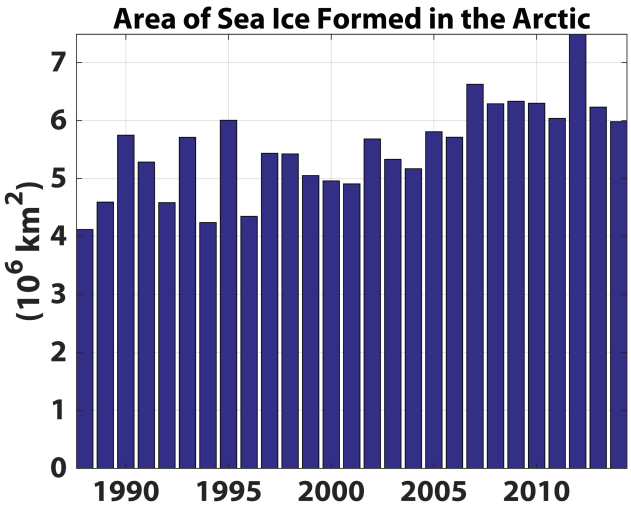

Figure 7. Area figure titles not always the same font size of sea ice formed each year in the Arctic in millions of square kilometers.

percent except for the last column, which lists the total area formed in each EEZ. The number of parcels is less than the total formed during the study period because some parcels were still "active" at the end of the study period and because there are some small areas that are between EEZs, but not properly part of the Central Arctic (see Figure 2).

The Russian shelves, known to be the "ice factory" of the Arctic [*Reimnitz et al*., 1994; *Timohkov*, 1994], dominate the ice-formation statistics, with over half of all sea-ice formation. Norway, the United States, and Canada follow, in that order. The dominant inter-EEZ fluxes are those that follow the two major ocean currents in the Arctic, the Beaufort Gyre and the Transpolar Drift Stream. Together they define a broad westward arc from North America toward Russia, westward past Norway, out of the Arctic through Fram Strait and along the eastern coast of Greenland. Thus, Canada exports ice to the United States, which exports to Russia, which exports to Norway. Nearly all Norwegian sea-ice melts within its own EEZ because warm North Atlantic waters meet ice-covered polar waters there. Even the smaller inter-EEZ transports are quite large. For example, the average transport from the Russian to the United States EEZ (a tiny fraction of Russian ice), is about 3,300 km^2 of sea ice each year.

We are interested in how these exchanges are shifting as the Arctic warms under the influence of increased greenhouse gas forcing. First, as noted above (Figure 3), receding summer ice cover has tended to increase the amplitude of the annual ice formation/melt cycle. Each winter, the sea-ice cover extends to the coastlines, so greater retreat in summer implies greater grow-back in the fall. The average annual Arctic-wide sea-ice formation in the years 2000–2014 was 17.4% higher than the average for 1988–1999 (5,993,208 km^2 vs. 5,045,104 km^2) (see Figure 7). In addition, fluxes between EEZs have tended to increase between the pre- and post-2000 time frames (Figure 8). As Figure 8 illustrates, fluxes from Russia to Norway and from Alaska to Russia, the two largest ice exporters, have increased by 11% and 16%, respectively. Some exports have

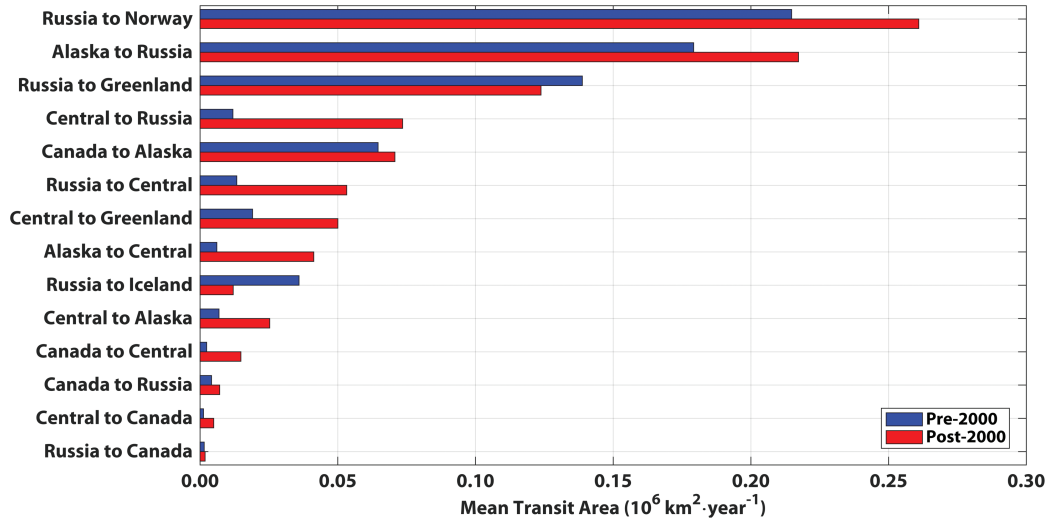

Figure 8. Annual flux of sea-ice area between exclusive economic zones, averaged over 1988–1999 (blue) and 2000–2014 (red).

Table 2. Annually Averaged Area of Sea Ice Transported Between EEZs: 1988–1999

To	Canada	USA	Russia	Norway	Iceland	Greenland	Central	Total
From	sq. km	sq. km	sq. km	sq. km	sq. km	sq. km	sq. km	sq. km
Canada	127,885	59,663	3,846	0	48	962	2,212	194,615
USA	1,346	201,779	165,433	0	769	8,365	5,625	383,317
Russia	1,394	1,827	2,422,163	198,269	33,173	128,125	12,308	2,797,260
Norway	0	0	625	626,731	96	5,481	0	632,933
Greenland	0	0	0	769	3,077	26,827	0	30,673
Central	1,154	6,346	11,010	5,433	3,702	17,596	8,798	54,038

EEZ, exclusive economic zones.

Table 3. Annually Averaged Area of Sea Ice Transported Between EEZs: 2000–2014

To	Canada	USA	Russia	Norway	Iceland	Greenland	Central	Total
From	sq. km	sq. km	sq. km	sq. km	sq. km	sq. km	sq. km	sq. km
Canada	143,393	75,804	7,634	0	0	0	15,893	242,723
USA	2,188	217,232	232,813	0	45	2,679	44,241	499,196
Russia	1,964	4,732	3,132,723	279,598	12,902	132,634	57,054	3,621,607
Norway	0	0	402	657,634	89	2,723	0	660,848
Greenland	0	0	0	1,652	1,786	18,929	0	22,366
Central	5,313	27,098	78,795	18,080	9,598	53,616	139,866	332,366

EEZ, exclusive economic zones.

declined, notably from Russia to Greenland and Iceland. Those declines are largely due to the very large increase in sea-ice melt in the Central Arctic as the melt front moves farther and more rapidly northward (Tables 2 and 3).

Figure 9 is a time series of ice transfer from Russia to North America (top) and from North America to Russia (bottom), binned by year of formation and averaged over a 5-year window. There is a general increasing trend, but there are also individual years that stand out above and below the trend, and there are significant reversals of the trend over several years.

That the trend in exchanges should be upward is not obvious from the overall trends in Arctic sea-ice patterns. On one hand, acceleration of sea ice (Figure 6) leads to shorter travel times between remote regions (Figure 10). Transit between most "trading partners" has shortened significantly. For example, Russian ice, reached its destinations in other nations' water an average of 46% faster while North American ice reached Eurasian waters an average of 37% faster. So too has the time for travel between the EEZs, which are mostly over the continental shelves, and the central Arctic Ocean. Shorter transit times should increase the inter-EEZ exchange by increasing the distance traveled before a parcel melts. However, the more extreme retreat of the summer ice edge—the increase in the size of the SIZ—has dramatically reduced the amount of first-year ice that survives to be "promoted" to multi-year ice. Thus, the fraction of multi-year ice has declined dramatically while the fraction of first-year ice has increased from about 50% to over 70% between the start of the satellite era and 2015 [*Perovitch et al.*, 2015]. Ice that melts in the same year as its formation is less likely to travel long distances than ice that survives summer and has another year on the move. The shift from multi-year to first-year ice might therefore diminish inter-EEZ exchanges. In the recent past, acceleration has dominated changes in inter-EEZ transport, which is increasing. At some future date, the summer melt may be so aggressive that the trend in transport reverses.

In addition, the increasing northward retreat of the ice edge creates a shift from ice formation over the shelf seas to the pelagic Central Arctic. The rapidity of the retreat—the ice edge now travels much farther each

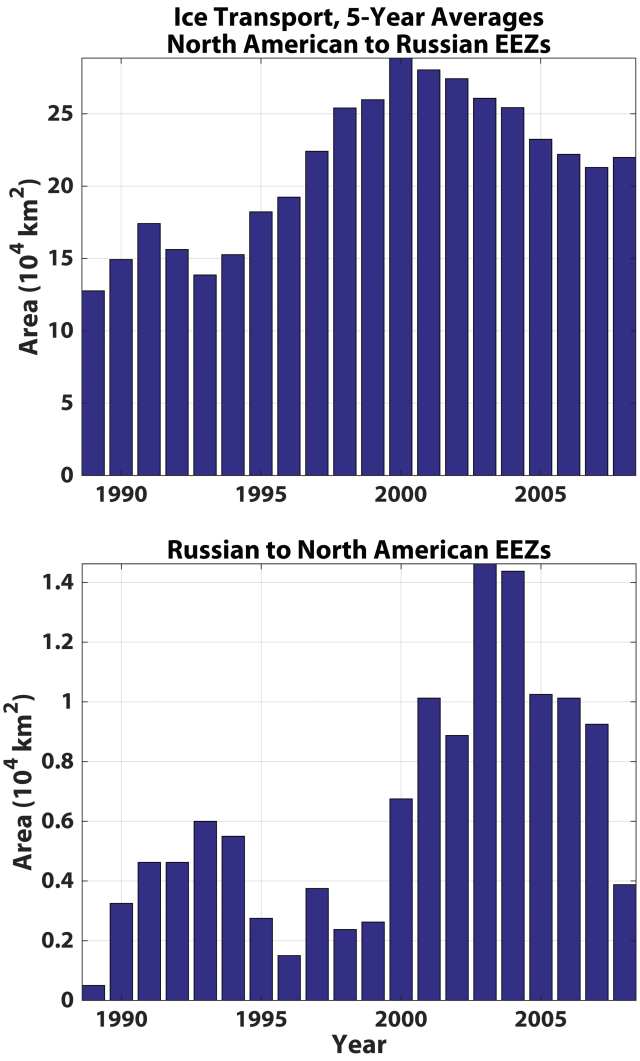

Figure 9. Five-year running average sea-ice area export from Russian to North American exclusive economic zones (top in 10^5 km^2) and vice versa (bottom in 10^4 km^2).

year during the same warm period—means that ice formed over the shelves is more likely to be caught by the melt front than previously. As a source of new sea-ice area, the Central Arctic increased by over 400% (310,208 km^2/yr between 2000 and 2014 vs. 58,542 km^2/yr in the 1988 and 1999 period). As a destination for ice formed in the EEZs, the increases were equally dramatic: over a sixfold increase in North American ice and 364% increase in ice from the Russian EEZ melting in the Central Arctic. Figure 11 tells part of the story: the spatial distribution of formation of sea-ice parcels that are eventually promoted to multi-year ice. Before 2000, multi-year ice mainly originated in the northern part of the EEZs. More recently, the largest contribution is from the Central Arctic while the region that produces only, or mainly, first-year ice has moved northward toward the EEZ's northern boundaries.

To understand the increase in inter-EEZ exchange despite the shift of multi-year ice formation out of the EEZs, we look at the distances traveled by first-year ice that travels from one EEZ to another (Figure 12: 1988–1999; blue: 2000–2014). The amount of first-year ice getting from one EEZ to another has grown dramatically (the blue area is 70% larger than the red in Figure 12); and the distances traveled tended to be longer—by 20% on average. Thus, even though the "lifespan" of Arctic sea ice is decreasing dramatically, it is traveling faster and melting at great distances more often, than before. *Spreen et al.* [2011] have shown that the sea-ice acceleration is partially, but not mainly, due to increased wind stress. Rather, the main effect must be an increased responsiveness of the ice pack to winds and ocean currents as a result of lower resistance as the ice thins and the ice area diminishes [*Tremblay et al.*, 2015].

4. Discussion and Future Work

In this contribution, we demonstrate that the LITS, based on the Polar Pathfinder sea-ice drift data set, can be used to visualize and understand exchanges in sea ice between Arctic regions. We apply the system to inter-EEZ transport during a period of strong climatic warming. The minimum ice extent is diminishing, which means that the ice edge is retreating farther north, and faster than in prior decades. As a result, ice formed over the continental shelves, which includes most of the EEZ area, must travel farther north to enter the perennial ice pack and the thick, multi-year ice is not being replenished at the rate at which it is being flushed out of the Arctic. We set out to answer the question: What would be the impact of these changes on exchange of sea ice between the waters of the Arctic nations. So far, the acceleration of sea ice is overcoming

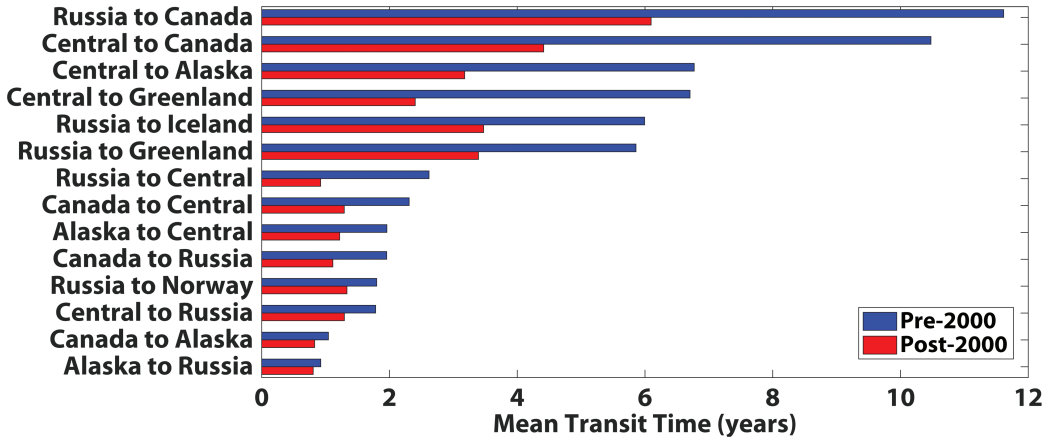

Figure 10. Change in transit time between formation time and melt time for ice flowing between pairs of exclusive economic zones. Blue: ice formed 1988–2000; red: ice formed 2001–2014.

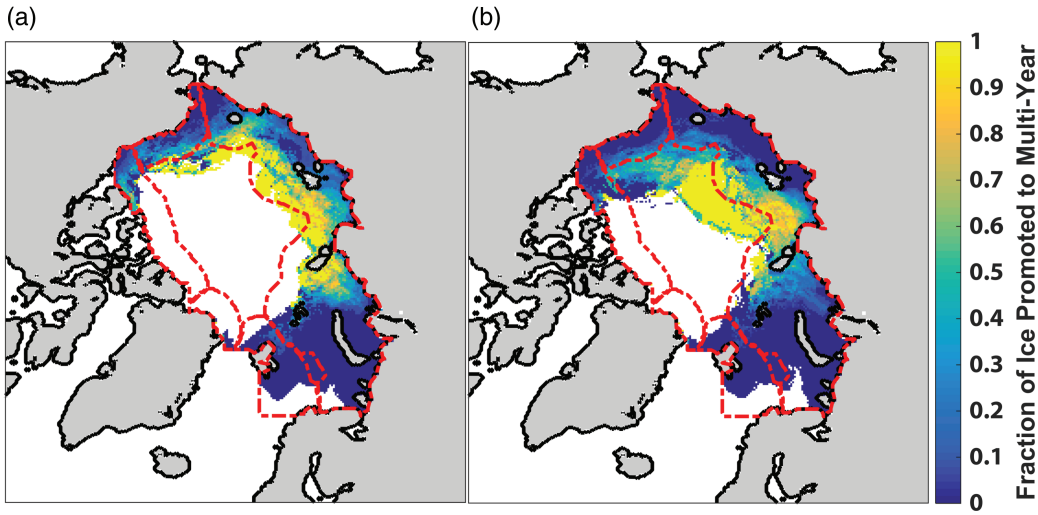

Figure 11. Spatial distribution of multi-year ice promotion for (a) why 1988? Different time span 1988–2000 and (b) 2000–2014. For each grid cell, fraction of the ice formed in that grid cell that melts more than 1 year after formation is shown. Exclusive economic zones boundaries are shown in red.

its shorter lifetime, and exchange between the EEZs, roughly corresponding to the continental shelf seas, has increased over the past 27 years. The increases are significant, both in the statistical sense and in that they are large—tens of thousands of square kilometers each summer.

In geopolitical terms, these developments draw the Arctic nations closer together. What happens in the Russian (or Canadian or United States) EEZ does not necessarily stay there. Rather, there is a wide, and widening, pathway capable of rafting large amounts of material from one EEZ to another. If there is an oil spill in the Chukchi (or Kara) Sea, it will necessarily be of great concern to Russia (or Norway), the downstream neighbor. If heavy metals are deposited downwind of smelters in Norilsk, then those responsible for fishing industries in Alaska and Norway must be concerned.

Most ice formed on the continental shelves nonetheless travels very little before it melts, so most contaminants introduced into sea ice will be released within the EEZ where the ice was formed. The risks of long-range ice rafting are modulated by the seasonality of ice transport and the specific drift conditions, especially at and immediately after incorporation into the ice. LITS, together with drift fields from Polar Pathfinder allows for estimation of the probability of long-distance ice rafting. To assess risks in a more

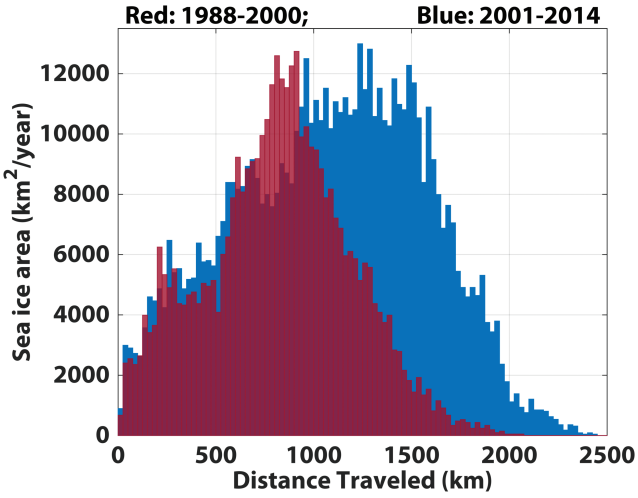

Figure 12. Distribution of distances traveled by first year? it takes longer than that no? Year ice transported between exclusive economic zones.

specific way, one would need to incorporate an ice-loading model together with information about specific times and places of inputs and releases, as well as vertical migration of material within an ice floe. For assessment of future risk, one would also need to integrate scenarios of future economic developments with these models of the physical system.

Another interesting shift is the dramatically increased exchange between the continental shelves and the central Arctic Ocean. As the summer ice pack shrinks, more ice formed in EEZs melts over the deep Arctic Ocean, and vice versa: more ice is formed over the pelagic regions of the central Arctic, which is for the first time a major formation site for new ice area. As the central Arctic opens up, a new biome is being created, which will be receiving ice-rafted material from several nation's waters, raising novel regulatory questions.

For the immediate future, continued fall and winter production of sea ice coupled with increases in ice speed is likely to mean that inter-EEZ transport continues. In a much warmer Arctic, when the summers are essentially ice free, more extensive summer melting could effectively cut-off some transport pathways. Analysis of climate projections is beyond the scope of this study, but is underway and will be presented in a separate paper. As we have pointed out elsewhere [*Newton et al.*, 2016], future sea-ice scenarios are critical for planning and policy development. For example, in planning for Arctic marine-protected areas it is important to consider how the supply from "ice-sheds" is likely to change [*Pfirman et al.*, 2010].

Acknowledgments
This work was funded through grants from the Office of Naval Research (N00014-11-1-0977) and National Science Foundation (ARC 06-33878 and PLR 15-04404). The project would not have been possible without the work of the NSIDC PolarPathfinder group to process satellite images of the Arctic Ocean into sea-ice drift vector fields. In particular, we have benefited from close interactions with Charles (Chuck) Fowler, Walt Meier, and Garrett Campbell. Data used in this paper can be accessed at the sources described in the Methods section.

References

Arctic Monitoring and Assessment Programme (1998), *AMAP Assessment Report: Arctic Pollution Issues*, xii + 859 pp., Arctic Monit. and Assess. Program. (AMAP), Oslo, Norway. [Available at http://www.amap.no/documents/doc/amap-assessment-report-arctic-pollution-issues/68.]

Arctic Monitoring and Assessment Programme (2011), *AMAP Assessment 2011: Mercury in the Arctic*, xiv + 193 pp., Arctic Monit. and Assess. Program. (AMAP), Oslo, Norway. [Available at http://www.amap.no/documents/doc/amap-assessment-2011-mercury-in-the-arctic/90.]

Arctic Monitoring and Assessment Programme (2015), *AMAP Assessment 2015: Black Carbon and Ozone as Arctic Climate Forcers*, vii + 116 pp., Arctic Monit. and Assess. Program. (AMAP), Oslo, Norway. [Available at http://www.amap.no/documents/doc/amap-assessment-2015-black-carbon-and-ozone-as-arctic-climate-forcers/1299.]

Barrie, L., E. Falck, D. Gregor, T. Iverson, H. Loeng, R. Macdonald, S. Pfirman, T. Skotvold, and E. Wartena (1998), The influence of physical and chemical processes on contaminant transport into and within the Arctic, in *AMAP Assessment Report: Arctic Pollution Issues*, edited by D. Gregor, L. Barrie, and H. Loeng , pp. 25–116 , Arctic Monit. and Assess. Program., Oslo, Norway.

Bauch, D., P. Schlosser, and R. Fairbanks (1995), An H218O study of the Arctic Ocean halocline and the sources of deep and bottom waters, *Prog. Oceanogr.*, *35*, 53–80. https://doi.org/10.1016/0079-6611(95)00005-2.

Bird, K.J., R.R. Charpentier, D.L. Gautier, D.W. Houseknecht, T.R. Klett, J.K. Pitman, T.E. Moore, C.J. Schenk, M.E. Tennyson and C.J. Wandrey (2008), *Circum-Arctic resource appraisal; estimates of undiscovered oil and gas north of the Arctic Circle*, 4 p., U.S.Geol. Surv. Fact Sheet 2008–3049. [Available at http://pubs.usgs.gov/fs/2008/3049/.]

Bischof, J. F., and D. A. Darby (1997), Mid- to late pleistocene ice drift in the Western Arctic Ocean: Evidence for a different circulation in the past, *Science*, *277*(5322), 74–78. https://doi.org/10.1126/science.277.5322.74.

Blanken, H., L. B. Tremblay, S. Gaskin, and A. Slavin (2017), Modeling the long-term evolution of worst-case Arctic oil spills, *Mar. Pollut. Bull.*, *116*(1–2), 315–331. https://doi.org/10.1016/j.marpolbul.2016.12.070.

DeCoste, L. (2016), *Canada Ups Its Arctic Game With Plans to Build a Port at the Top of the World*, Vice News, 4/8/2016. [Available at https://news.vice.com/article/canada-ups-its-arctic-game-with-plans-to-build-port-at-the-top-of-the-world.]

DeRepentigny, P., L.-B. Tremblay, R. Newton, and S. Pfirman (2016), Patterns of sea-ice retreat in the transition to a seasonally ice-free Arctic, *J. Clim.*, *29*(19), 6993–7008. https://doi.org/10.1175/jcli-d-15-0733.1.

Dethleff, D., V. Rachold, M. Tintelnot, and M. Antonow (2000a), Sea-ice transport of riverine particles from the Laptev Sea to Fram Strait based on clay mineral studies, *Int. J. Earth Sci.*, *89*, 496–502. https://doi.org/10.1007/s005310000109.

Dethleff, D., H. Nies, I. H. Harms, and M. J. Karcher (2000b), Transport of radionuclides by sea-ice and dense-water formed in western Kara Sea flaw leads, *J. Mar. Syst.*, *24*, 233–248. https://doi.org/10.1016/s0924-7963(99)00088-3.

Drozdowski, A., S. Nudds, C. G. Hannah, H. Niu, I. K. Peterson, and W. A. Perrie (2011), Review of Oil Spill Trajectory Modelling in the Presence of Ice, *Can. Tech. Rep. Hydrogr. Ocean Sci.*, *274*, 84 pp., Bedford Institute of Ocean Science, Bedford, Canada.
Eicken, H., E. Reimnitz, V. Alexandrov, T. Martin, H. Kassens, and T. Viehoff (1997), Sea-ice processes in the Laptev Sea and their importance for sediment export, *Cont. Shelf Res.*, *17*(2), 205–233. https://doi.org/10.1016/s0278-4343(96)00024-6.
Eicken, H., J. Kolatschek, J. Freitag, F. Lindemann, H. Kassens, and I. Dmitrenko (2000), A key source area and constraints on entrainment for basin-scale sediment transport by Arctic sea ice. *Geophys. Res. Lett.*, *27*(13), 1919–1922. https://doi.org/10.1029/1999GL011132.
Emery, W. J., C. W. Fowler, J. Hawkins, and R. H. Preller (1991), Fram strait satellite image-derived ice motions, *J. Geophys. Res.*, *96*(C3), 4751–4768. https://doi.org/10.1029/90JC02273.
Emery, W., C. Fowler, and J. Maslanik (1995), in *Satellite Remote Sensing of Ice Motion, in Oceanographic Applications of Remote Sensing*, edited by M. Ikeda and F. W. Dobson, CRC Press, Boca Raton, Fla.
Emery, W. J., C. W. Fowler, and J. A. Maslanik (1997), Satellite-derived maps of Arctic and Antarctic sea-ice motion, *Geophys. Res. Lett.*, *24*(8), 897–900. https://doi.org/10.1029/97GL00755.
Fowler, C., W. J. Emery, and J. Maslanik (2004), Satellite derived Arctic sea ice evolution Oct. 1978 to March 2003, *IEEE Geosci. Remote Sens. Lett.*, *1*(2), 71–74. https://doi.org/10.1109/lgrs.2004.824741.
Gautier, D. L., et al. (2009), Assessment of undiscovered oil and gas in the Arctic, *Science*, *324*, 1175–1179. https://doi.org/10.1126/science.1169467.
Harvey, F., and Walker 2013, Arctic oil spill is certain if drilling goes ahead, says top scientist, *The Guardian*. [Available at www.theguardian.com/world/2013/nov/19/arctic-oil-drilling-russiaHastings.]
Jakobsson, M., R. Løvlie, E. M. Arnold, J. Backman, L. Polyak, J.-O. Knutsen, and E. Musatov (2001), Pleistocene stratigraphy and paleoenvironmental variation from Lomonosov Ridge sediments, central Arctic Ocean, *Global Planet. Change*, *31*(1–4), 1–22. https://doi.org/10.1016/s0921-8181(01)00110-2.
Khelifa, A. (2010), A summary review of modelling oil in ice, in *Arctic and Marine Oilspill Program Technical Seminar 33*, pp. 587–608.
Khon, V. C., I. I. Mokhov, M. Latif, V. A. Semenov, and W. Park (2010), Perspectives of Northern Sea Route and Northwest Passage in the twenty-first century, *Clim. Change*, *100*, 757. https://doi.org/10.1007/s10584-009-9683-2.
Kwok, R., A. Schweiger, D. A. Rothrock, S. Pang, and C. Kottmeier (1998), Sea ice motion from satellite passive microwave imagery assessed with ERS SAR and buoy motions, *J. Geophys. Res.*, *103*(C4), 8191–8214. https://doi.org/10.1029/97JC03334.
Meibing, J., C. Deal, J. Wang, V. Alexander, R. Gradinger, S.-I. Saitoh, I. Takahiro, Z. Wan, and P. Stabeno (2007), Ice-associated phytoplankton blooms in the southeastern Bering Sea, *Geophys. Res. Lett.*, *34*, L06612. https://doi.org/10.1029/2006GL028849.
National Academies of Science (NAS) (2014), *Responding to Oil Spills in the U.S. Arctic Marine Environment*. [Available at http://nap.edu/18625.]
Newton, R., P. Schlosser, D. G. Martinson, and W. Maslowski (2008), Freshwater distribution in the Arctic: Results from simulation with a high-resolution model and model-data comparison, *J. Geophys. Res. Oceans*, *113*(C05024). http://doi.org/10.1029/2007JC004111.
Newton, R., P. Schlosser, R. Mortlock, J. Swift, and R. MacDonald (2013), Canadian basin freshwater sources and changes: Results from the 2005 Arctic Ocean section, *J. Geophys. Res. Oceans*, *118*, 2133–2154. https://doi.org/10.1002/jgrc.20101.
Newton, R., S. Pfirman, P. Schlosser, B. Tremblay, M. Murray, and R. Pomerance (2016), White Arctic vs. Blue Arctic: A case study of diverging stakeholder responses to environmental change, *Earth's Future*, *4*(8), 396–405. https://doi.org/10.1002/2016EF000356.
National Snow and Ice Data Center (NSIDC) (2016), *Ice Motion from Passive Microwave: SMMR, SSM/I, SSMIS and AMSR-E*. [Available at: https://nsidc.org/data/docs/daac/nsidc0116_icemotion/smmr_ssmi.html#accuracy.]
Nürnberg, D., I. Wollenburg, D. Dethleff, H. Eicken, H. Kassens, T. Letzig, E. Reimnitz, and J. Thiede (1994), Sediments in Arctic sea ice: Implications for entrainment, transport and release, *Mar. Geol.*, *119*, 185–214. https://doi.org/10.1016/0025-3227(94)90181-3.
Perovitch, D., W. Meier, M. Tschudi, S. Farrell, S. Gerland, and S. Hendricks (2015), Sea ice, in *The Arctic Report Card: Update for 2015*. [Available at http://www.arctic.noaa.gov/Report-Card/Report-Card-2015/ArtMID/5037/ArticleID/217/Sea-Ice.]
Pfirman, S., M. Lange, I. Wollenburg, and P. Schlosser (1990), Sea ice characteristics and the role of sediment inclusions in deep-sea deposition, in *Geologic history of the polar oceans: Arctic versus Antarctic*, edited by U. Bleil and J. Thiede, pp. 187–211, NATO ASI Series C, Kluwer Academic, Amsterdam, Neth.
Pfirman, S. L., H. Eicken, D. Bauch, and W. F. Weeks (1995), The potential transport of pollutants by Arctic sea ice, *Sci. Total Environ.*, *159*, 129–146. https://doi.org/10.1016/0048-9697(95)04174-y.
Pfirman, S., B. Tremblay, R. Newton, and C. Fowler (2010). The Last Arctic Sea Ice Refuge, American Geophysical Union, Fall Meeting abstract #C43E-0592. American Geophysical Union, Washington, DC.
Rampal, P., J. Weiss, and D. Marsan (2009), Positive trend in the mean speed and deformation rate of Arctic sea ice: 1979–2007, *J. Geophys. Res.*, *114*, C05013. https://doi.org/10.1029/2008JC005066.
Rampal, P., J. Weiss, C. Dubois, and J.-M. Campin (2011), IPCC climate models do not capture Arctic sea ice drift acceleration: Consequences in terms of projected sea ice thinning and decline, *J. Geophys. Res.*, *116*, C00D07. https://doi.org/10.1029/2011JC007110.
Reimnitz, E., D. Dethleff, and D. Nurnberg (1994), Contrasts in the Arctic shelf sea-ice regimes and some implications: Beaufort Sea versus Laptev Sea, *Mar. Geol.*, *119*, 215–225. https://doi.org/10.1016/0025-3227(94)90182-1.
Ruskin, L. (2016), *Murkowski: Where's That Arctic Port? Alaska Public Media*. [Available at http://www.alaskapublic.org/2016/03/02/murkowski-seeks-funding-for-deep-water-port-in-alaska/.]
Schwegmann, S., C. Haas, C. Fowler, and R. Gerdes (2011), A comparison of satellite-derived sea-ice motion with drifting-buoy data in the Wedell Sea, *Ann. Glaciol.*, *52*(57), 103–110. https://doi.org/10.3189/172756411795931813.
Shevchenko, V. P., A. A. Vinogradova, A. P. Lisitzin, A. N. Novigatky, M. V. Panchenko, and V. V. Pol'kin (2012), Aeolian and ice transport of matter (including pollutants) in the Arctic, in *Implications and Consequences of Anthropogenic Pollution in Polar Environments*, edited by R. Kallenborn , pp. 59–74 , Springer-Verlag, Berlin; Heidelberg, Germany.
Smith, L. C., and S. R. Stephenson (2013), New Trans-Arctic shipping routes navigable by midcentury, in *Proceedings of the National Academy of Sciences*, edited by E. S. Mosley-Thompson, *100*(13), E1191–E1196. https://doi.org/10.1073/pnas.1214212110.
Sørstrøm, S. E., P. J. Brandvik, I. Buist, P. Daling, D. Dickins, L.-G. Faksness, S. Potter, J. F. Rasmussen, and I. Singsaas (2010), *Oil in Ice – JIP, Report 32: Joint Industry Program on Oil Spill Contingency for Arctic and Ice-Covered Waters, Summary Report, SINTEF A14181. Open*, isbn:978-82-14-02759-2, SINTEF, Trondheim, Norway.
Spreen, G., R. Kwok, and D. Menemenlis (2011), Trends in Arctic sea ice drift and the role of wind forcing: 1992–2009, *Geophys. Res. Lett.*, *38*, L19501. https://doi.org/10.1029/2011GL048970.
State of Alaska, Department of Transportation (2016), *Arctic Port Study*. [Available at http://www.dot.state.ak.us/stwddes/desports/arctic.shtml.]

Thorndike, A. S., and R. Colony (1982), Sea ice motion in response to geostrophic winds, *J. Geophys. Res.*, *87*(C8), 5845–5852. https://doi.org/10.1029/JC087iC08p05845.

Timohkov, L. A. (1994), Regional characteristics of the Laptev and the East Siberian Seas: Climate, topography, ice phases, thermohaline regime, circulation, in *Russian-German Cooperation in the Siberian Shelf Seas: Geo-System Laptev Sea*, edited by H. Kassens, H-W Hubberten, S. M. Pryamikov, and R. Stein, pp. 15–31 , Alfred Wegener Inst. for Polar and Mar. Res., Bremerhaven, Germany.

Tremblay, L. B., G. A. Schmidt, S. Pfirman, R. Newton, and P. DeRepentigny (2015), Is ice-rafted sediment in a North Pole marine record evidence for perennial sea-ice cover? *Philos. Trans. R. Soc. A*, *373*(2052). https://doi.org/10.1098/rsta.2014.0168.

Tschudi, M., C. Fowler, J. Maslanik, J. S. Stewart, and W. Meier (2016). *Polar Pathfinder Daily 25 km EASE-Grid Sea Ice Motion Vectors. Version 3*. Boulder, Colo.: Natl. Snow and Ice Data Cent.. 10.5067/O57vait2Ayyy.

Venkatesh, S., H. El-Tahan, G. Comfort, and R. Abdelnour (1990), Modelling the behavior of oil spills in ice-infested waters, *Atmos. Ocean*, *28*(3), 303–329. https://doi.org/10.1080/07055900.1990.9649380.

Williams, J., L.-B. Tremblay, R. Newton, and R. Allard (2016), Dynamic preconditioning of the September sea-ice extent minimum, *J. Clim.*